ORIGINAL ARTICLE

Biosorption of copper, lead and nickel on immobilized *Bacillus coagulans* using experimental design methodologies

Dai-yin Lei · Zhuan Liu · Yu-hong Peng · Shou-bin Liao ·
Heng Xu

Abstract Biosorption of copper, lead and nickel onto immobilized *Bacillus coagulans* (IBC) from aqueous solution in single- and multi-metal systems was investigated. The results of scanning electron microscopy coupled with energy dispersive X-ray analysis (SEM-EDXA) and Fourier transform infrared (FTIR) spectrometry demonstrated the importance of surface morphology and identified the active groups involved in adsorption. In batch studies, the most significant factors were screened by Minimum Run Res V Design. The Simplex Lattice Mixture Design was then successfully applied to explore the maximum adsorption capacity of the three metals (75.3 mg/g for copper, 118.3 mg/g for lead and 68.4 mg/g for nickel) and the preferential adsorption of IBC followed the order: Pb (II)> Cu (II)>Ni (II). Furthermore, adsorption kinetics and adsorption isotherms of single-, binary-, and ternary-metal systems were studied and the experimental data was found to fit well to the Freundlich isotherm and pseudo-second-order kinetics.

Keywords *Bacillus coagulans* · Heavy metal · Simplex lattice design · Selective adsorption

Introduction

Heavy metals, released from a variety of industries including electroplating, nickel-cadmium batteries, steel fabrication and so

D.-y. Lei · Z. Liu · H. Xu (✉)
Key Laboratory of Bio-resources and Eco-environment (Ministry of Education), College of Life Science, Sichuan University,
Chengdu, Sichuan 610064, China
e-mail: xuheng64@sina.com

Y.-h. Peng
Yaan Vacational College, Yaan 625000, People's Republic of China

S.-b. Liao
Shiling Subdistrict Office of Longquanyi District, Longquan,
Chengdu, Sichuan 610106, China

on, are causing huge threats to the environment and public health due to their toxicity, non-biodegradability and bio-accumulation (Kumar et al. 2009). Metals such as copper, nickel and lead are the most frequently discharged among heavy metals. The excessive ingestion of heavy metals by living organisms has toxic effects, for example vomiting, cramps, convulsions, serious lung and kidney problems or even death (He et al. 2005; Fu and Wang 2011). In addition, lead can accumulate in the kidney and liver, disrupting basic cellular processes and nervous system (Fu and Wang 2011; El-Sayed 2013).

In recent years, a number of conventional and advanced technologies including cationic exchange resin, electrolytic treatment (Hunsom et al. 2005), membrane technology (Yang and Kocherginsky 2006), precipitation (Soylak and Erdogan 2006; Uluozlu et al. 2010), solvent extraction (Borowiak-Resterna et al. 2010), reverse osmosis (Eloussaief and Benzina 2010), and adsorption (Dai et al. 2010; Chen et al. 2011) have been employed to remove heavy metals from wastewater (Nassar et al. 2004; Kobya 2004). Among all the methods, biosorption has the inherent advantages of low operating cost, efficiency, selectivity and environmental friendliness, and is known as the most useful and potential alternative technique for metal removal (Ozturk 2007; Özdemir et al. 2009). To date, hundreds of adsorbents, such as activated carbon (Moreno-Piraján et al. 2010), fungi (Kumar et al. 2008), *Lentinus edodes* (Liu et al. 2011), and *Saccharomyces cerevisiae* (El-Sayed 2013) have been reported. Among the different adsorbents, bacteria such as *Streptomyces* (Saurav and Kannabiran 2011) and the marine cyanobacteria (Rajeshwari et al. 2012) show excellent metal-binding properties due to their cell wall construction (Fan et al. 2008). *Bacillus* such as *Bacillus cereus*, *B. licheniformis*, *B. subtilis*, *B. pumilus* and *B. thuringiensis*, have already been tested as potential materials for removing toxic metals (Çolak et al. 2011).

However, there are some difficulties in the application of simple bacteria due to particle size, mechanical strength and rigidity. Thus, the need for innovation in treatment technologies for water contaminated with these metals is urgent.

Immobilization of microorganisms within a polymeric matrix can resolve some of the drawbacks and provide greater opportunity for reuse (Vijayaraghavan and Yun 2008). Immobilization of microbial cells is used successfully in domestic and industrial wastewater treatments (Juarez Jimenez et al. 2012). Furthermore, there are some reports in the literature of immobilization being used in continuous and semi-continuous wastewater treatment systems (Fenice et al. 2000). Some natural polymers such as alginate, chitosan and chitin are used as immobilization matrices as they are efficient, inexpensive and non-toxic. In addition, alginates are used widely as immobilization matrices to remove heavy metals from wastewater (Arıca et al. 2001; Bayramoğlu et al. 2006). In this study, alginate was used to immobilize *Bacillus coagulans* for wastewater treatment. All the experiments were conducted on a laboratory scale only without real industrial effluents to establish the foundations of practical application. Our aim was to study the adsorption of Cu (II), Pb (II) and Ni (II) by immobilized *B. coagulans* (IBC).

Materials and methods

Microorganisms, medium and cultivation

The bacterial strain of *B. coagulans* used in this study was kindly donated by the microbiology laboratory of Sichuan University (Cheng Du, China). The bacterium was cultured on Luria-Bertani (LB) agar medium containing 0.5 % yeast extract, 1 % tryptone, 1 % NaCl and 1.5–2 % agar, and stored at 4 °C for further use after being cultivated for 24 h.

Cultivation of *B. coagulans* used in metal sorption was carried out in 250 mL Erlenmeyer flasks with 100 mL LB broth (pH 7.0) on a rotary shaker at 200 rpm and 37 °C for 24 h. Cells were harvested by centrifugation, washed several times with deionized water and kept at 4 °C until use.

Preparation of immobilized cell beads

Immobilization of *B. coagulans* was carried out as follows: a mixture of 2 % (w/v) sodium alginate solution and commensurable wet *B. coagulans* cells was extruded through a 2.5 mL syringe into 0.5 mol (M) CaCl$_2$ solutions, then stirred slowly for polymerization and bead formation. The pellets (2 mm in diameter) were hardened in the same solution overnight at 4 °C, and then collected via filtration, rinsed thoroughly with deionized water, and finally dried at room temperature for use in subsequent experiments.

Reagents and apparatus

All chemicals and reagents used for adsorption were purchased from Kelong (ChengDu, China) and were of guaranteed grade. Stock solutions (1,000 mg/L) of Cu (II), Pb (II) and Ni (II) were

prepared by dissolving a certain amount of Cu(NO$_3$)$_2$·3H$_2$O, Pb(NO$_3$)$_2$ and Ni(NO$_3$)$_2$·6H$_2$O in deionized water; these solutionw were acidified slightly with HNO$_3$ (1–2 drops of pure aqua fortis), and then kept in the dark at 25 °C. The standard solutions used in the following experiments were achieved by diluting the exact quantity of stock solutions with deionized water, respectively.

The pH was measured by a pH meter (Model, pHS-25). The analysis of the metal concentration in the remaining aqueous solution was determined by flame AA-220Fs Atomic Absorption Spectrometer (Varian, Palo Alto, CA).

Characterization of adsorbent

The surface morphology and elemental constituents of the biosorbent before and after biosorption were studied by scanning electron microscopy coupled with energy dispersive X-ray analysis (JSM-5900LV, JEOL, Tokyo, Japan). In order to detect the functional groups that might be related to the uptake of heavy metal ions, Fourier transform infrared (FTIR) spectrometer (NEXUS-650, Thermo Electron Scientific Instruments, Madison, WI) was employed to collect the spectra within a range of 400–4,000 cm^{-1}.

Experimental design

To improve the systematic implementation and ease of this experiment, this study used the program Design-Expert 7.0.0 (Stat-Ease, Minneapolis MN), which furnishes both experimental design and data analysis including Minimum (Min) Run Res V design and simplex lattice mixture design (SLMD).

Min Run Res V design

Min Run Res V design—a standard two-level factorial design—identified efficiently not only the main variables but also two-factor interactions with the minimum number of runs. In the present research, Min Run Res V design was used to evaluate variables that affected the uptake of heavy metals of Cu (II), Pb (II) and Ni (II) in a single-metal system. Six independent variables (pH, initial metal ions concentration, biomass loading, contact time, temperature and agitation speed) were considered to obtain the removal rate (%) of the three heavy metals, respectively.

Simplex lattice mixture design

As a standard mixture design, SLMD was used to investigate the different affinity of three toxic metals with IBC in complex wastewater. In this design model, all variables had the same range and were dependent on each other while the sum of the variables was constant. Besides the characteristics above, enough points to estimate a full cubic model were also

displayed in the experiments. In order to analyze the lack of fit, this design was augmented with axial check blends and an overall centroid to increase the size of the test to a total of 14 combinations for the three factors [primary components of Cu (II), Pb (II) and Ni (II)] as shown in Table 1.

Batch adsorption studies

A series of batch tests was conducted by shaking a specified amount of adsorbent in conjunction with 50 mL metal solution at the desired concentration using a shaker incubator (SUKUN, SKY-211B) at 200 rpm. After adsorption, the samples were filtered and the supernatants measured for residual Cu (II), Pb (II) and Ni (II) concentrations. For the aims of this study, batch sorption studies were performed as follows:

> Adsorption kinetics: to investigate the adsorption mechanism, 0.1 g sorbent with initial ion concentration of 50 mg/L in solution at pH 6 was shaken at 200 rpm and 25 °C. Samples were taken at different time intervals, from 5 to 540 min.
> Sorption isotherms: the isotherms experiment was accomplished by mixing 0.1 g IBC with seven different initial concentrations of metal ion solution ranging from 10 to 200 mg/L at pH 6.0 while stirring at 25 °C and 200 rpm for 9 h, respectively.

Because most industrial effluents contain mainly mixtures of toxic metals, competitive biosorption of Cu (II), Pb (II) and Ni (II) ions was studied. Binary and ternary mixtures of ions were processed in the same way as described for single metal solutions. All tests were carried out in triplicate and the mean values are presented as the results. The removal rate (%) of metal ions and the adsorption capacity were computed using following equations:

$$\text{Removal rate } (\%) = 100 \times (C_0 - C_e)/C_0 \tag{1}$$

$$\text{Adsorption capacity } (mg/g) : q_e = (C_0 - C_e)/M \tag{2}$$

Where C_0 and C_e are the initial and final concentration (mg/L) of heavy metals, respectively; q_e is the adsorption capacity (mg/g); and M is adsorbent dosage (g/L).

Results and discussion

SEM-EDXA images

SEM and EDXA of pellets before and after metal adsorption are shown in Fig. 1. Compared with the pristine beads shown in Fig. 1a, the surface of the adsorbent became smoother after

adsorption as shown in Fig. 1b, because the metals were adsorbed onto *B. coagulans* and the surface structure might be damaged by the incursion of copper, lead and nickel. The EDXA further confirms the adsorption of heavy-metal ions onto the adsorbent (Chen et al. 2011). The EDXA pattern (Fig. 1a) shows that the surface of the pristine (unloaded) beads contained elements of C, O, Cl and Ca, whereas the surface of the beads (Fig. 1b) contained elements of C, O, Cu, Pb and Ni. The result indicates that calcium ions take part in the adsorption process via ion exchange with copper, lead and nickel.

FTIR spectra

To further investigate the chemical characterization of the sorbents and the interaction between the functional groups of the beads and metal ions, FTIR spectra was used to characterize the biosorbents structurally (Gerbino et al. 2011). Figure 2 shows typical FTIR spectra of *B. coagulans* before and after metal uptake. The similarities seen in the spectra indicated that the components and structure of *B. coagulans* were still intact. Nonetheless, changes in the absorption peaks suggested the presence of functional groups responsible for the adsorption process. For pure *B. coagulans* (spectrum *a* in Fig. 2), the broad band at 3,431 cm^{-1} was assigned to −OH stretching vibrations in carboxylic acid and −NH$_2$ stretching (Munagapati et al. 2010; Chen et al. 2011). The bands at 1,616 and 1,423 cm^{-1} could be attributed to –COO– antisymmetrical and symmetrical stretching of carboxylate ions, respectively (Yan et al. 2010). The stretching vibration polysaccharides was at 1,200–800 cm^{-1} (Zhang et al. 2011). In addition, the bands present below 800 cm^{-1} were in the fingerprint zone of phosphate and sulfur functional groups (Munagapati et al. 2010). As can be seen from spectrum *b* in Fig. 2, after interaction with metal ions, the peak intensities at 1,616, 1,423, 696 and 625 cm^{-1} decreased, meanwhile the bands changed at 1,014 cm^{-1}. These results demonstrated that carboxyl, hydroxyl, amine, –CO, polysaccharides and phosphate and sulfur groups probably participated in the sorption process.

Identification of significant factors by Min Run Res V design

The layout of six variables designed by Min Run Res V along with the responses of Cu (II), Pb (II) and Ni (II) removal rate (%) is shown in Table 2. A wide variation was found, ranging from 1.10 %, 7.47 % and 5.71 % to 87.50 %, 98.42 % and 38.68 % for Cu (II), Pb (II) and Ni (II), indicating that different conditions produced different and large effects on metal removal. The adequacy of the models and the significant variables were tested via ANOVA (Table 3). The Model *F*-values of Cu (II) (23.30), Pb (II) (26.29), Ni (II) (10.26) and the Prob>*F* values were less than 0.05, implying that these models and the model terms were significant. The R^2_{Pred} of 0.7924, 0.8134 and 0.5775 were in reasonable agreement with the R^2_{Adj} of 0.8643, 0.8784 and 0.7258 for Cu (II), Pb (II) and

Table 1 Simplex lattice mixture design (SLMD) matrix of three mixture metal contents of 75 mg/L, 150 mg/L, 300 mg/L and the adsorption capacities of *Bacillus coagulans*

No.	Metal concentration (75 mg/L)			Metal concentration (150 mg/L)			Metal concentration (300 mg/L)			Experimental uptake (mg/g)		
	Cu	Pb	Ni	Cu	Pb	Ni	Cu	Pb	Ni	Cu	Pb	Ni
1	0	75	0							0	37.4	0
2	37.5	37.5	0							16.2	18.3	0
3	0	37.5	37.5							0	18.7	7.9
4	37.5	37.5	0							16.0	18.3	0
5	50	12.5	12.5							21.4	6.1	2.8
6	25	25	25							10.9	12.3	5.6
7	0	75	0							0	37.4	0
8	75	0	0							32.8	0	0
9	12.5	50	12.5							5.4	24.3	2.4
10	12.5	12.5	50							5.6	6.1	12.4
11	0	0	75							0	0	21.4
12	37.5	0	37.5							16.4	0	8.8
13	75	0	0							33.7	0	0
14	0	0	75							0	0	21.3
15				75	0	75				22	0	15
16				25	100	25				7.7	47.5	5.2
17				0	0	150				0	0	34.3
18				150	0	0				40.2	0	0
19				100	25	25				27.8	11.5	5.5
20				75	75	0				21.3	32.9	0
21				0	150	0				0	71.4	0
22				50	50	50				15.2	23.7	10.8
23				0	150	0				0	70.7	0
24				0	75	75				0	36.1	18.2
25				0	0	150				0	0	35.5
26				75	75	0				21.4	33.2	0
27				150	0	0				40.9	0	0
28				25	25	100				7.9	12.2	21.8
29							0	0	300	0	0	68.4
30							150	0	150	41.2	0	31.8
31							0	150	150	0	51.6	30.2
32							300	0	0	74.7	0	0
33							50	50	200	15.5	21.2	42.7
34							0	0	300	0	0	67.3
35							150	150	0	39.6	53.2	0
36							50	200	50	14.5	78.1	10.1
37							100	100	100	29.8	41.7	21.4
38							300	0	0	75.3	0	0
39							150	150	0	39.3	53.6	0
40							0	300	0	0	118.3	0
41							200	50	50	53.3	20.5	10.9
42							0	300	0	0	117.9	0

Ni (II), respectively. Meanwhile, the R^2 values were 0.9031 for Cu (II), 0.9132 for Pb (II), 0.8041 for Ni (II), which is a measure of how well the regression model fit. Meanwhile, to measure adequate precision, the signal to noise ratios were 17.644, 17.759 and 11.349 (the value greater than 4 is desirable). To sum up, these models can help researchers navigate

Fig. 1 Scanning electron
microscopy (oscopy (SEM)
images and energy dispersive X-
ray analysis (EDXA) of
immobilized *Bacillus coagulans*
(IBC). **a** Before adsorption, **b** after
Cu (II), Pb (II) and Ni (II)
adsorption
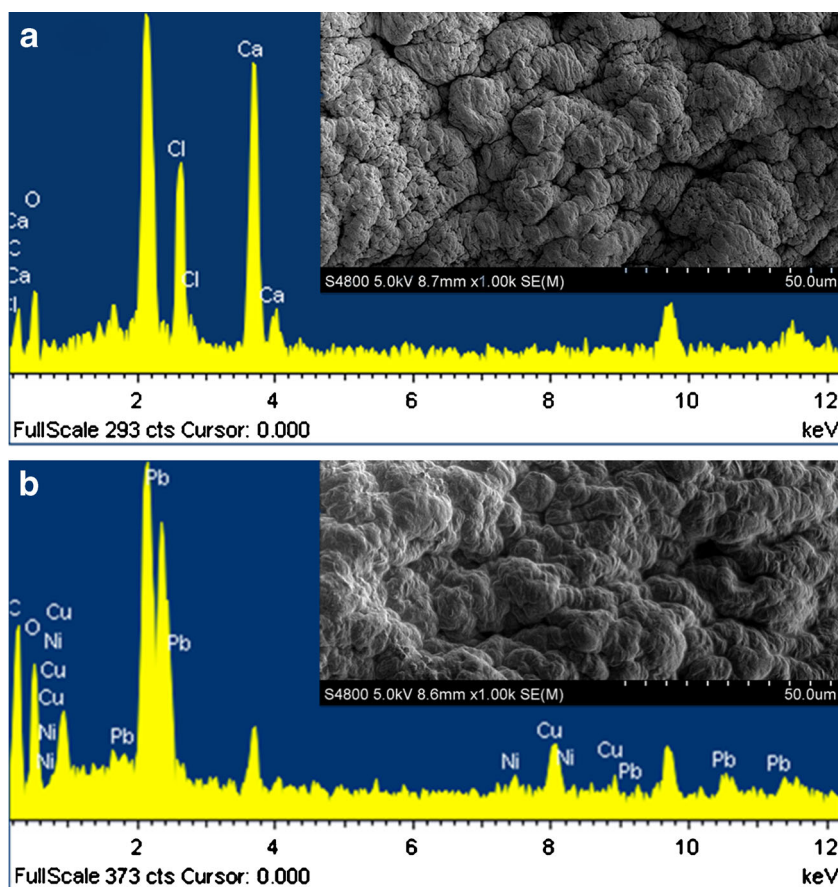
the design space. The optimum equations in terms of coded
factors obtained by Min Run Res V design are given below:

$$Cu\ removal\ (\%) = +33.30 + 0.19*A + 11.23*B - 2.47*C \quad (3)$$
$$+ 6.35*D + 16.40*E + 7.13*F$$

$$Pb\ removal\ (\%) = +57.50 + 2.36*A + 10.11*B - 3.79*C \quad (4)$$
$$+ 5.53*D + 21.79*E + 8.10*F$$

$$Ni\ removal\ (\%) = +18.37 - 0.55*A + 5.67*B + 2.60*C \quad (5)$$
$$+ 2.53*D + 4.80*E + 2.05*F$$

Where A, B, C, D, E and F stand for the coded values
defined in Table 1. According to Eqs. (3)–(5), the main factors
affecting the removal rate were deduced as pH, biomass
loading, contact time, agitation speed for Cu (II) and Pb (II),
while the main factors for Ni (II) were pH, initial metal ions
concentration, biomass loading, and contact time.

In order to perceive the main effects more intuitively, the
results analyzed by main effects were plotted with regard to their
effects on removal rate (Fig. 3). The two extreme points were
selected and the other factors were set at a middle value. For
example, using the software to examine the pH factor, the values
of temperature, initial metal ions concentration, biomass loading,

contact time, agitation speed are 30, 55, 4, 155 and 125, respec-
tively. It was observed that the slope of the line could directly
reveal the relative importance of the effects of various factors.
Thus, factors pH, biomass loading, contact time and agitation
speed performed more importantly for Cu (II) and Pb (II) re-
moval, while factors such as pH, initial metal ion concentration,
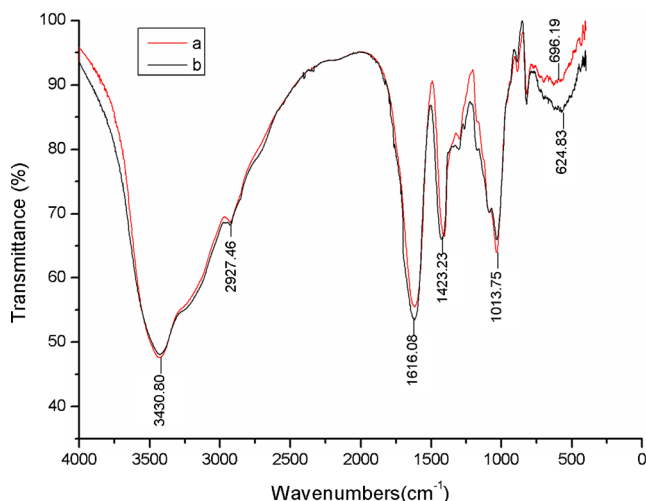biomass loading and contact time were more important for Ni (II)

Fig. 2 Fourier transform infrared (FTIR) spectra of *Bacillus coagulans*
native (*line a*) biomass and heavy-metal ions loaded (*line b*) biomass

Table 2 The Minimum (Min) Run Res V design matrix of six variables and the responses of Cu (II), Pb (II) and Ni (II) respectively

Run	Factors						Responses (% removal)		
	Temperature (°C)	pH	Initial metal ions (mg/L)	Biomass loading (mg/L)	Contact time (min)	Agitation speed (rpm)	Cu	Pb	Ni
1	40	2	10	6	300	50	34.93	77.44	11.13
2	20	2	10	2	300	50	29.72	55.09	7.05
3	20	6	10	6	10	200	37.55	72.00	15.94
4	20	2	100	2	300	200	28.17	61.97	17.26
5	40	6	100	2	10	200	20.62	41.67	19.53
6	40	2	100	6	300	200	50.08	91.97	23.14
7	40	6	100	2	300	50	30.73	62.37	24.42
8	20	2	10	2	10	200	1.47	19.78	7.38
9	20	2	100	6	10	200	19.98	38.03	18.93
10	20	6	100	2	10	50	16.03	32.77	17.28
11	40	6	100	6	10	50	22.60	35.77	20.29
12	20	2	10	6	10	50	1.10	12.72	5.71
13	20	6	10	2	300	200	79.20	94.23	31.98
14	40	6	10	6	300	200	87.50	98.42	38.68
15	40	6	10	2	10	50	16.32	57.20	10.70
16	40	2	10	2	300	200	38.78	86.53	10.43
17	20	6	10	6	300	50	60.52	84.54	31.24
18	40	2	100	2	10	50	4.55	7.47	15.59
19	40	2	10	6	10	200	24.90	39.08	7.53
20	40	6	100	2	10	50	16.33	31.40	13.53
21	20	6	100	6	300	200	70.33	96.47	33.51
22	20	2	100	6	300	50	41.27	68.00	22.98

removal, which is the same result as that obtained by evaluation with Eqs. (3)–(5). With this test, temperature, pH, biomass loading, contact time and agitation speed had a positive relationship to Cu (II) and Pb (II) removal. A similar trend for pH and biomass loading was found previously to have positive effects on the removal of Pb (II) (Liu et al. 2011). For Ni (II), together with the residual factors, it was the initial metal ion concentration rather than the temperature that showed a positive effect. On the contrary, the initial metal ion concentration performed negatively relative to the removal of Cu (II) and Pb (II), while temperature was negative for Ni (II). According to the above conclusions, a temperature of 25 °C, pH 6, biomass loading of 2 g/L, and an agitation speed of 200 rpm were chosen for subsequent tests.

Data analysis from SLMD

The experimental design for each of the three metals (SLMD for a polynomial of the third order) and results are given in Table 1. With the help of Design-Expert Software, the model predicted for the response variable was a quadratic mixture model, which was demonstrated to be significant (F-value: 6,419.60 for Cu(II), 17,767.45 for Pb (II), 17,77.22 for Ni (II) and P-value<0.0001). The coefficient of determination (R^2)

of the model was 0.9998, 0.9999 and 0.9991 for Cu (II), Pb (II) and Ni (II), respectively, indicating a good fit for the responses. The values of lack-of-fit [1.82 for Cu (II), 1.22 for Pb (II) and 1.64 for Ni (II)] were far greater than the desired 0.05, which implied that the quadratic mixture model was relatively adequate for the predicted aim.

A graphical representation for the biosorption of Cu (II), Pb (II) and Ni (II) onto IBC in a ternary system with a total metal concentration of 150 mg/L is shown in Fig. 4. From the triangular contour diagrams in Fig. 4 (a_1)–(a_3), it can be seen that the uptake of target metal by IBC was influenced by the other coexisting metal ions, with interference being in the order Pb (II)>Ni (II), Cu (II)>Ni (II) and Pb (II)>Cu (II), resulting in an adsorption preference of *B. coagulans* of: Pb (II)>Cu (II)>Ni (II). Triangular three-dimensional diagrams are also shown in Fig. 4 (b_1)–(b_3) . The actual experimental points (solid dots) essentially corresponded to the predicted surfaces plots, indicating that SLMD was valid for the present research and could predict the behavior of multi-metal adsorption well. However, the concentration of industrial effluents was indeterminate. To strengthen the feasibility of this work in practical applications, multi-metal biosorption with a lower total concentration (75 mg/L) and a higher total concentration

Table 3 ANOVA of Cu (II), Pb (II) and Ni (II) ion removal for Min Run Res V variables fitted to factorial model

Metal ion	Source	Sum of squares	df	Mean square	F-value	P-value Prob>F		R^2	R^2_{Adj}	R^2_{Pred}	Adequate precision
Cu	Model	10,722.33	6	1,787.05	23.30	< 0.0001	Significant	0.9031	0.8643	0.7924	17.644
	A	0.80	1	0.80	0.01	0.9201					
	B	2,691.21	1	2,691.21	35.09	< 0.0001					
	C	130.33	1	130.33	1.70	0.2120					
	D	860.21	1	860.21	11.22	0.0044					
	E	5,735.48	1	5,735.48	74.78	< 0.0001					
	F	1,085.03	1	1,085.03	14.15	0.0019					
Pb	Model	15,284.57	6	2,547.43	26.29	< 0.0001	Significant	0.9132	0.8784	0.8134	17.759
	A	118.63	1	118.63	1.22	0.2860					
	B	2,180.67	1	2,180.67	22.50	0.0003					
	C	305.84	1	305.84	3.16	0.0959					
	D	651.52	1	651.52	6.72	0.0204					
	E	10,124.70	1	10,124.70	104.48	< 0.0001					
	F	1,398.41	1	1,398.41	14.43	0.0017					
Ni	Model	1,462.52	6	243.75	10.26	0.0001	Significant	0.8041	0.7258	0.5772	11.349
	A	6.40	1	6.40	0.27	0.6113					
	B	684.80	1	684.80	28.83	< 0.0001					
	C	144.38	1	144.38	6.08	0.0262					
	D	136.48	1	136.48	5.75	0.0300					
	E	492.23	1	492.23	20.72	0.0004					
	F	89.81	1	89.81	3.78	0.0708					

(300 mg/L) was also studied using SLMD. As can be seen from Figs. 5 and 6, the trends of competitive adsorption [Pb (II)>Cu (II)>Ni (II)] were consistent with those observed in previous tests, with a total metal concentration of 150 mg/L. Similar response surface plots from model simulation were observed for the adsorption of Cu (II), Pb (II) and Ni (II), which corresponded perfectly to the experimental data, suggesting a high coherence among the dependent variables. Contrasting the results in Figs. 5 and 6 and the results in Fig. 4, there was no difference on the shape of the triangular three-dimensional surface with the three different total metal concentrations (75, 150 and 300 mg/L). This result implied that the interaction of the target metal with its co-existing metal ions in the ternary sorption system was similar regardless of the difference in total metal concentration. Nevertheless, another interesting finding observed in Fig. 5a,b was that the black lines (experimental data) were nearly parallel to the white lines (predicted single-metal system), suggesting that the Cu (II) and Pb (II) adsorption were less affected by co-existing metal ions at the lower total metal concentration of 75 mg/L. The results were probably due to the abundant functional groups available for binding and the electronegativity of the metal ion.

In the present research, the maximum metal adsorption capacities of *B. coagulans* (shown in Table 1) were found to be 75.3, 118.3 and 68.4 mg/g for copper, lead and nickel, respectively. Futalan et al. (2011) found the highest capacity of

chitosan immobilized on bentonite as 20.90, 28.77 and 12.35 mg/g for copper, lead and nickel, respectively. The biosorption capacity of *Aspergillus niger* biomass obtained for Ni (II) was 1.6 mg/g and Pb (II) was 4.7 mg/g (Amini and Younesi 2009). As a result, *B. coagulans* had a relatively significant potential for removing these metal ions from effluents.

Adsorption kinetics for single and multiple-metal solutions

To investigate the type of adsorption mechanism from the reaction modalities and reaction rate constants, three popular kinetic models were utilized, namely the pseudo-first-order model (Eq. 6), pseudo-second-order model (Eq. 7) and Elovich model (Eq. 8) (Murugesan et al. 2011):

$$\ln(q_e - q_t) = \ln q_e - k_1 t \qquad (6)$$

$$\frac{t}{q_t} = 1/(k_2 q_e^2) + t/q_e \qquad (7)$$

$$q_t = (1/y)\ln(xy) + (1/y)\ln t \qquad (8)$$

Where q_e (mg/g) and q_t (mg/g) are the biosorption capacity of *B. coagulans* at equilibrium at time t (min); k_1 (min^{-1}) and k_2 (g/mg min) are the pseudo-first-order and pseudo-second-order

Fig. 3 Main effects plot for removal of **a** Cu (II), **b** Pb (II) and **c** Ni (II) by IBC
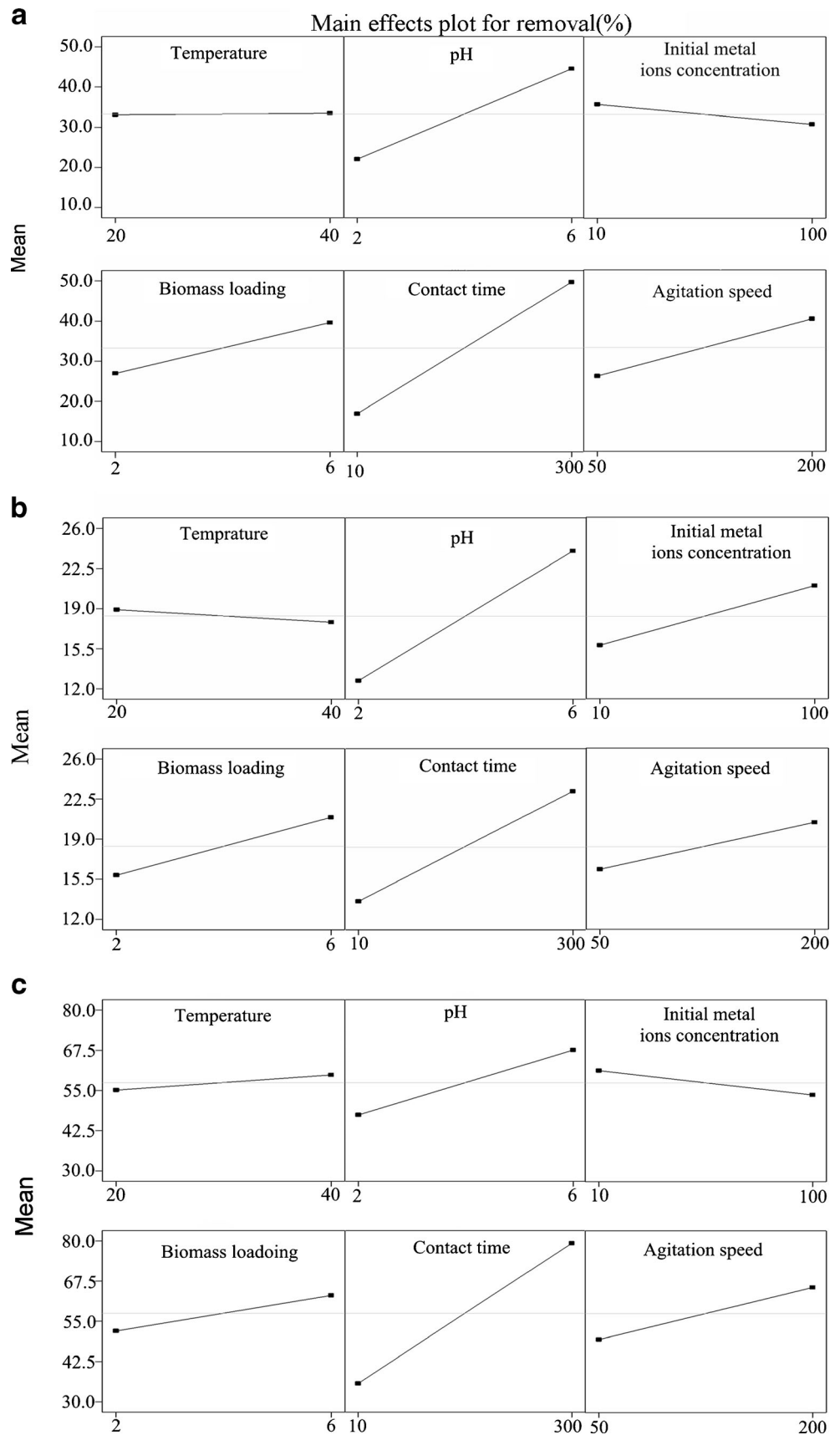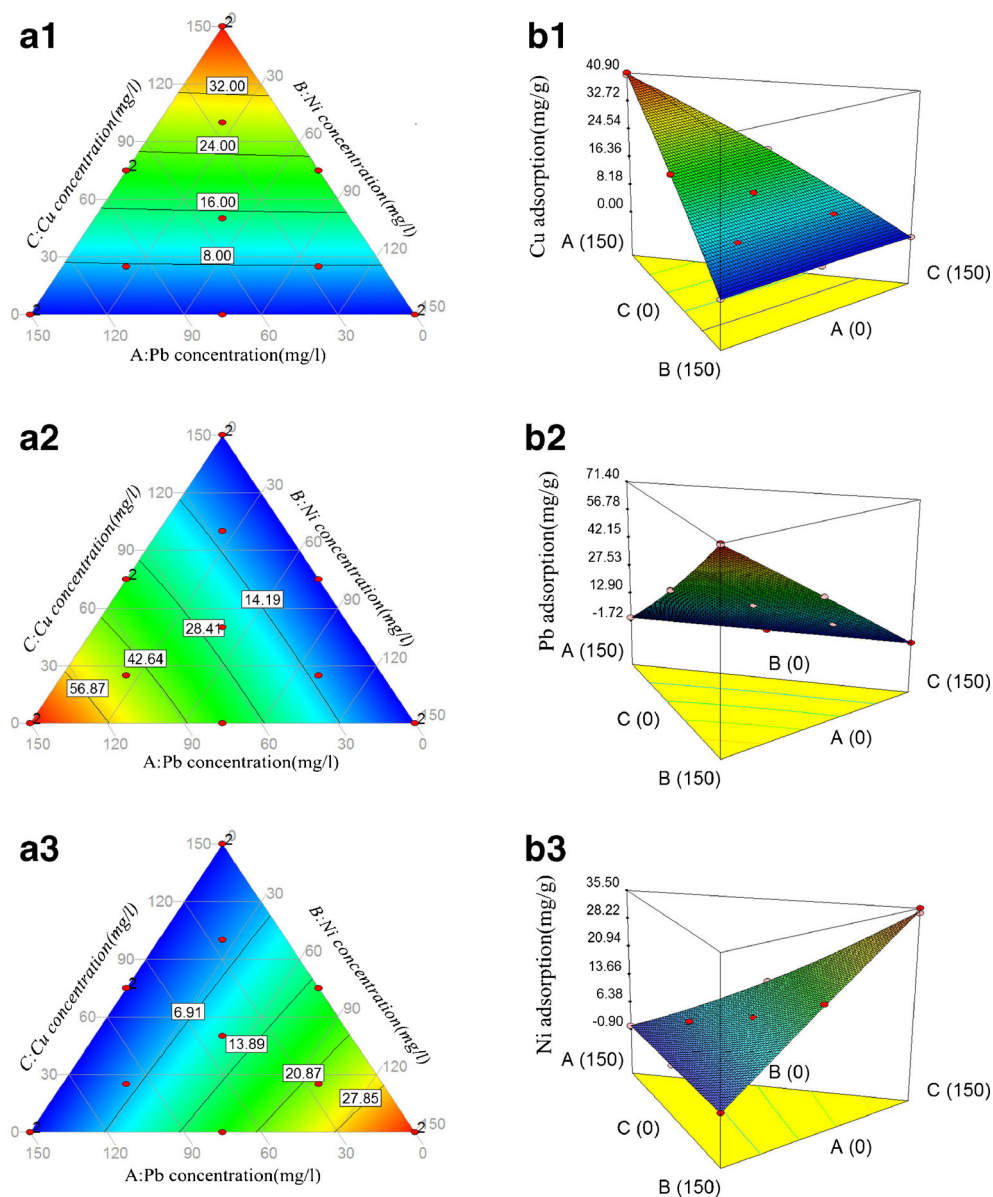
Fig. 4 Graphical representation of the biosorption of Cu (II), Pb (II) and Ni (II) onto IBC in a ternary system. **a** Triangular contour diagrams, and **b** triangular three-dimensional biosorption surfaces: the total metal concentration was 150 mg/L; the values indicated in (a₁), (a₂) and (a₃) were biosorption capacities in units of mg/g


rate constants, respectively; x and y are known as the Elovich coefficients: x stands for the initial sorption rate (mg/g min) and y is related to the activation energy of chemisorption (g/mg) in the surface coverage.

The rate constant, adsorption capacity and correlation coefficients (R^2) calculated from linear regressive Eqs. (6), (7) and (8) are listed in Table 4. The conformity between the values calculated by the model and the experimental data were confirmed by the correlation coefficient (R^2). Compared with the pseudo-first-order and the Elovich models, the pseudo-second-order model had the highest R^2 values, implying that chemisorption played a leading role in the adsorption progress. Moreover, the q_e calculated by Eq. (7) were very close to the experimental results, which further demonstrated that the

sorption rate of the three metals was followed by pseudo-second-order kinetics. In the single metal adsorption system, the q_e (exp) followed the order Pb (II)>Cu (II)>Ni (II), while the adsorption capacity values in the binary and ternary metal adsorption systems also followed the same selective order. Similar results were found in comparative and competitive adsorption of copper, lead, and nickel using chitosan immobilized on bentonite (Futalan et al. 2011). Moreover, the adsorption capacities in multi-metal systems decreased considerably compared to a single system, suggesting a strong competition among metal ions in binding to the active groups of IBC. In addition, the different adsorption rates might be related to competition among the metals for active groups on *B. coagulans*.

Fig. 5 Graphical representation of the biosorption of Cu (II), Pb (II) and Ni (II) onto IBC in a ternary system. **a** Triangular contour diagrams, and **b** triangular three-dimensional biosorption surfaces: the total metal concentration was 75 mg/L; the values indicated in (a_1), (a_2) and (a_3) were biosorption capacities in units of mg/g
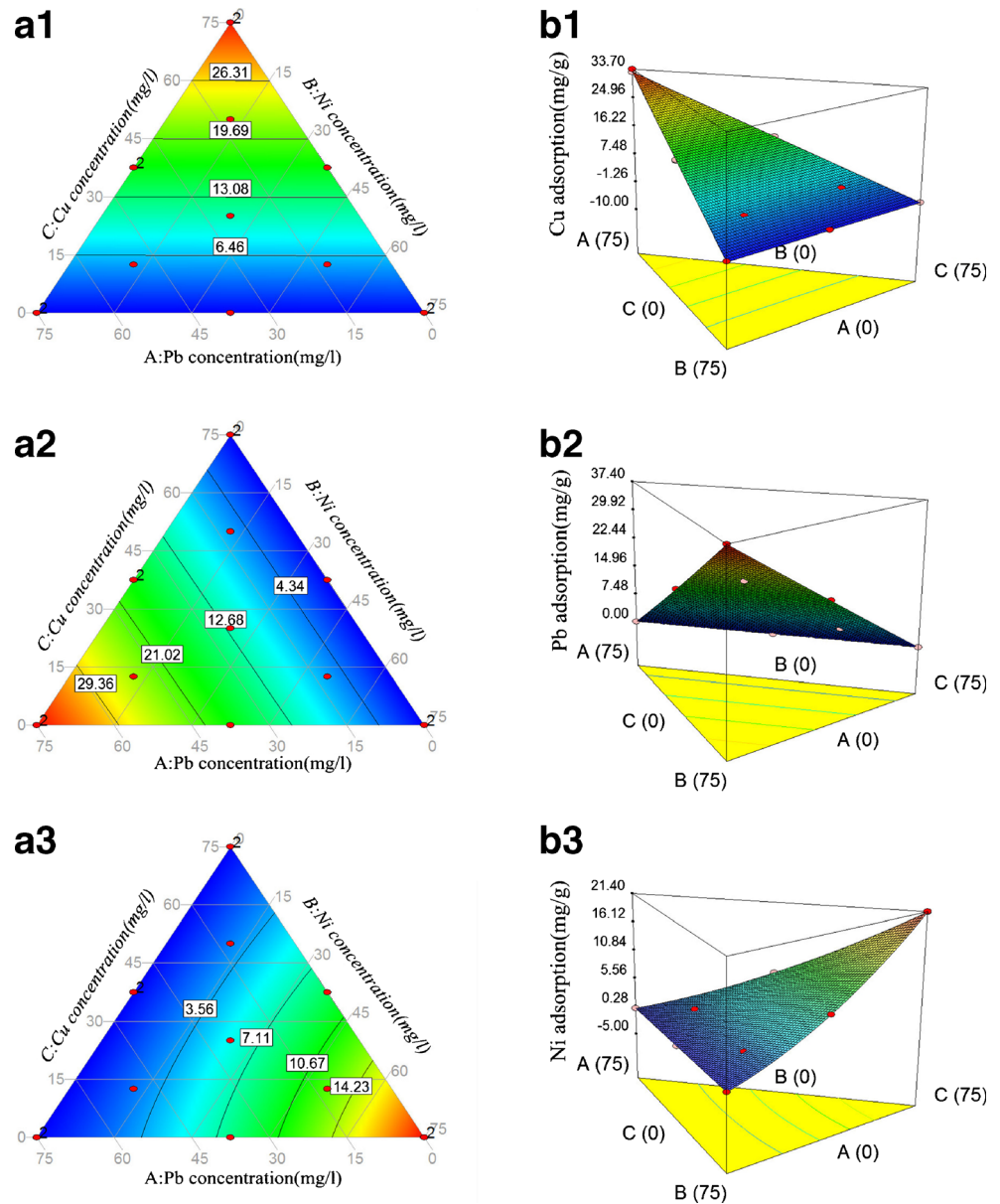
## Adsorption isotherms for single- and multiple-metal solutions

Adsorption isotherms, which are needed for designing an optimal adsorption process for industrial application, were employed to calculate the capacity of *B. coagulans*. The Langmuir isotherm model (Özdemir et al. 2009) assuming a homogenous adsorption surface with binding sites, gave equal energies as the linear form in Eq. (9):

$$\frac{c_e}{q_e} = 1/(q_m K_L) + C_e/q_m \qquad (9)$$

Where q_e and q_m are the adsorption capacity (mg/g) and the maximum adsorption capacity (mg/g) of the heavy metal at equilibrium, respectively. C_e is the equilibrium concentration (mg/L) of the metal ions in solution, and K_L represents the Langmuir constant related to the affinity between the metal ions and the binding sites of the adsorbents. In addition, the Freundlich equation and the Temkin isotherm were also used to investigate the adsorption equilibrium, expressed as:

$$\ln q_e = \ln K_F + (1/N)\ln c_e \qquad (10)$$

Fig. 6 Graphical representation of the biosorption of Cu (II), Pb (II) and Ni (II) onto IBC in a ternary system. **a** Triangular contour diagrams, and **b** triangular three-dimensional biosorption surfaces: the total metal concentration was 300 mg/L; the values indicated in (a₁), (a₂) and (a₃) were biosorption capacities in units of mg/g
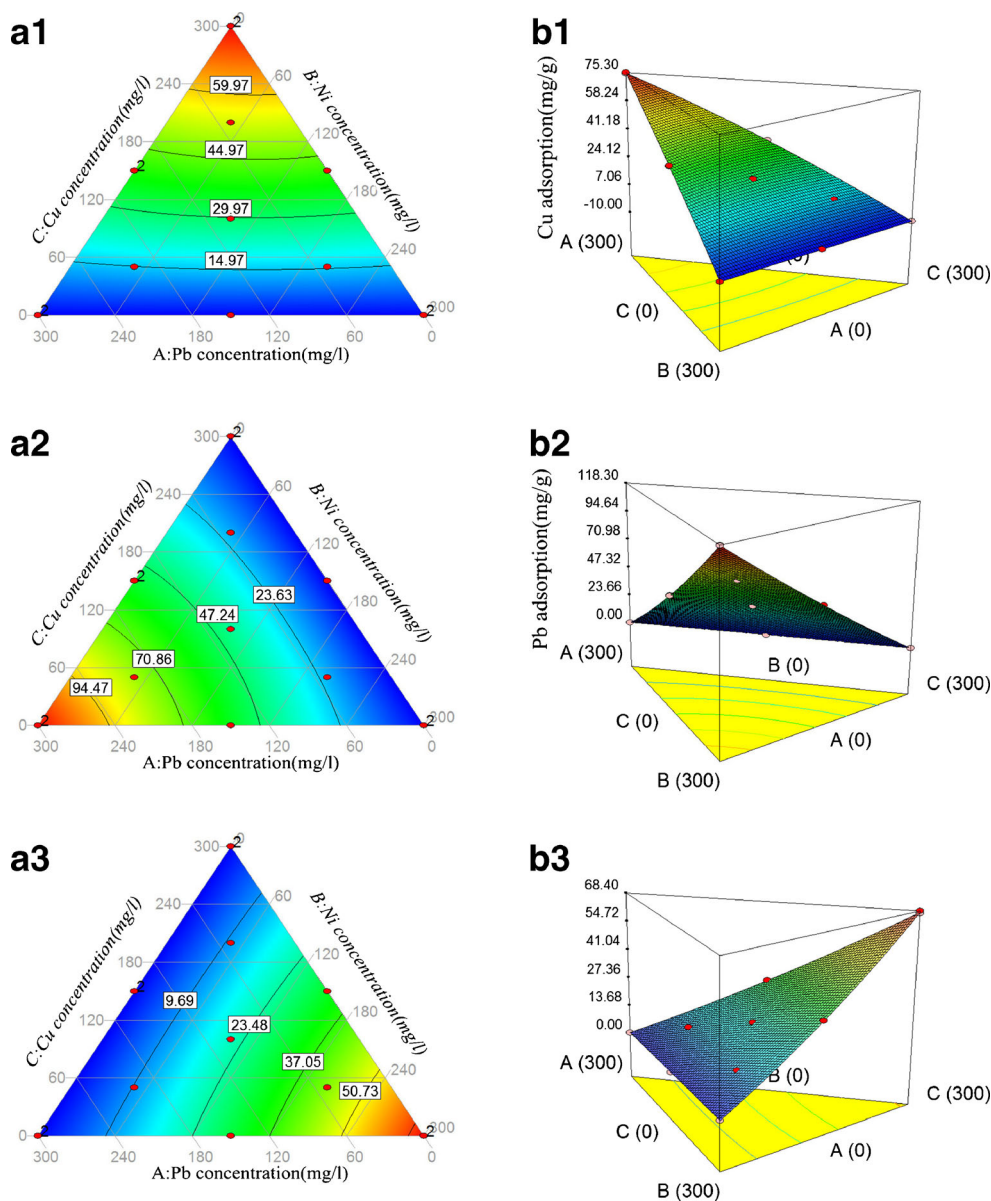
$$q_e = (RT/b)\ln c_e + (RT/b)\ln K_T \qquad (11)$$

Where q_e (mg/g) and c_e (mg/L) are the same as Eq. (9), K_F (mg/g) is the adsorption capacity and N (a value greater than 1 is desired) is the Freundlich constant related to the adsorption intensity; b (J/mol) is the Temkin isotherm constant related to the heat of biosorption, K_T (L/mg) is the Temkin isotherm constant, R is the universal gas constant (8.314 J/mol), while T(K) represents the absolute temperature.

In Table 5, the Langmuir, Freundlich, and Tempkin parameters are summarized along with correlation coefficients. As can be noted, the three metals in single- and multi-metal solution systems had the highest correlation coefficients (R^2) for the Freundlich isotherm model, indicating that the adsorption isotherms were better fitted to Freundlich model than to the Langmuir and Temkin models. The reason may be that adsorption took place on the heterogeneous surface of IBC and the sorption capacity of sorbents was less restricted by the Freundlich model (Zhao et al. 2011). As an indicator of adsorption intensity, N values ranging from 1.27 to 3.24 indicated that the adsorption process was favorable. The comparison of K_F for the three metals in the single metal systems showed that the affinity of the metal ions bound to IBC followed the order Pb (II)>Cu (II)>Ni (II). For the binary system, K_F was in the order Cu (II)>Ni (II), Pb (II)>Ni (II) and Pb (II)>Cu (II), while in the ternary metal system, lead had a higher K_F (10.39) than copper

Table 4 A comparison of kinetic parameters of single, binary and tertiary metal systems

			Pseudo-first-order			Pseudo-second-order			Elovich			q_e (exp)
			q_{e1}(cal) (mg g^{-1})	k_1 (min^{-1})	R^2	q_{e2} (cal) (mg g^{-1})	k_2 (g mg^{-1} min^{-1})	R^2	x (mg g^{-1} min^{-1})	y (mg g^{-1})	R^2	(mg g^{-1})
Single metal system		Cu	8.52	0.009	0.979	15.15	3.11×10^{-3}	0.999	4.80	0.52	0.978	15.00
		Pb	14.11	0.010	0.900	25.00	2.27×10^{-3}	0.999	8.68	0.29	0.981	24.06
		Ni	1.43	0.008	0.928	14.08	27.06×10^{-3}	1.000	7.52×10^{8}	1.80	0.926	14.47
Binary metal system	Cu-Ni	Cu	9.58	0.004	0.986	14.49	1.05×10^{-3}	0.992	0.58	0.44	0.969	13.61
		Ni	0.97	0.001	0.180	12.66	19.69×10^{-3}	0.998	2.83×10^{21}	4.59	0.506	12.94
	Cu-Pb	Cu	12.45	0.013	0.760	14.93	3.58×10^{-3}	0.998	12.50	0.56	0.996	14.48
		Pb	16.81	0.008	0.948	23.81	1.28×10^{-3}	0.998	2.60	0.25	0.995	22.56
	Ni-Pb	Ni	2.41	0.005	0.954	12.82	10.65×10^{-3}	0.999	1.42×10^{7}	1.62	0.993	12.25
		Pb	20.37	0.013	0.974	25.64	1.52×10^{-3}	0.999	3.66	0.25	0.985	23.83
Tertiary metal system		Cu	5.36	0.009	0.963	12.82	5.12×10^{-3}	0.998	22.93	0.79	0.980	12.76
		Pb	15.09	0.007	0.990	22.73	1.08×10^{-3}	0.996	2.02	0.26	0.995	21.33
		Ni	1.65	0.007	0.943	11.76	17.23×10^{-3}	0.999	2.06×10^{12}	2.80	0.957	11.38

(4.21) and nickel (0.7). In this case, the adsorption of heavy metals was suppressed by the presence of co-existing metals in the solution and an antagonistic influence on the adsorption capacity was exerted by the metals (Murugesan et al. 2011). Furthermore, that binary metal systems follow the Langmuir and Freundlich adsorption isotherm model was also discovered by Futalan et al. (2011).

Selectivity of IBC in removing Cu, Pb and Ni

Based on the above-mentioned conclusions in single and multi-metal systems, it emerged that Pb (II) had the highest adsorption capacity compared to Cu (II) and Ni (II) under the same conditions. Yan et al. (2010) showed that copper and zinc were very similar in molecular mass (63.57 and 65.38 g/mol), ionic radius (73 and 74 pm) and electronegativity (1.90 and 1.65 Pauling). Therefore, the Cu (II) had an advantage over Ni (II). In addition, these similarities between two metal ions enhanced their competition for the same active sites on cell walls and consequently lessened the competitive effect of each other on lead (Yan et al. 2010). Moreover, Pb (II) had a greater affinity than Cu (II) and Ni (II) in the mixture solution. These properties might be attributed to the electronegativity, the standard reduction potential and other physicochemical properties of metal ions (Vijayaraghavan et al. 2009). Therefore, the selective adsorption of IBC followed the order Pb (II)>Cu (II)>Ni (II).

Table 5 Adsorption isotherm model constants of single, binary and tertiary metal systems

			Langmuir			Freundlich			Temkin		
			q_m(cal) (mg g^{-1})	K_L (L mg^{-1})	R^2	K_F (mg g^{-1} (L mg^{-1})$^{1/N}$)	N	R^2	K_T (L mg^{-1})	b (J mol^{-1})	R^2
Single metal system		Cu	526.32	0.0041	0.9688	4.86	2.40	0.9879	0.06	16300	0.8933
		Pb	357.14	0.0347	0.8588	19.91	2.83	0.9914	10.59	204	0.9912
		Ni	120.48	0.0064	0.9024	1.22	1.35	0.9993	0.24	234	0.8951
Binary metal system	Cu-Ni	Cu	42.19	0.1007	0.9797	3.20	2.23	0.9894	4.74	14669	0.9784
		Ni	94.34	0.0043	0.8562	0.65	1.27	0.9993	0.17	293	0.8856
	Cu-Pb	Cu	22.99	0.8932	0.9720	3.62	2.88	0.9922	0.18	8413	0.9502
		Pb	125.00	0.0643	0.9873	12.43	2.87	0.9929	11.82	338	0.9473
	Ni-Pb	Ni	67.57	0.0089	0.9060	1.11	1.47	0.9975	0.23	317	0.9039
		Pb	212.77	0.0510	0.9687	12.83	2.40	0.9988	9.69	256	0.9638
Ternary metal system		Cu	51.28	0.2742	0.9847	4.21	3.24	0.9926	0.03	6723	0.9444
		Pb	114.94	0.0714	0.9907	10.39	2.62	0.9923	6.21	316	0.9624
		Ni	60.98	0.0060	0.8348	0.70	1.39	0.9960	0.18	365	0.8842

Conclusions

The adsorption performance of IBC together with comparative and competitive adsorption of Cu (II), Pb (II) and Ni (II) onto IBC were analyzed via batch experiments in single- and multi-metal systems. The following conclusions were drawn:

(1) The experimental results showed IBC to be a effective adsorbent for Cu (II), Pb (II) and Ni (II) removal from wastewater. The SEM-EDXA images of IBC showed that the heavy metals [Cu (II), Pb (II), Ni (II)] had been adsorbed onto the biosorbents, with Ca^{2+} disappearing and the surface morphology of *B. coagulans* changed obviously after metal uptake.

(2) FTIR spectroscopy proved that carboxyl, hydroxyl, amine, polysaccharides and phosphate and sulfur groups probably participated in the sorption process.

(3) Min Run Res V design studies with six variables indicated that the main factors affecting the removal rate of Cu (II) and Pb (II) were pH, biomass loading, contact time, agitation speed; while pH, initial metal ions concentration, biomass loading and contact time were the key factors in the removal rate of Ni (II). The maximum adsorption capacity of IBC for the three metals (75.3 mg/g for Cu, 118.3 mg/g for Pb and 68.4 mg/g for nickel) followed the order: Pb (II)>Cu (II)>Ni (II), which was the same as the selective order of IBC proved in the mixture design.

(4) The equilibrium sorption data in single- and multi-metal systems fit quite well to a pseudo-second-order kinetic model and Freundlich isotherm model, indicating that chemisorption controlled the adsorption rate.

References

Amini M, Younesi H (2009) Biosorption of Cd (II), Ni (II) and Pb (II) from aqueous solution by dried biomass of *Aspergillus niger*. Application of response surface methodology to the optimization of process parameters. Clean Soil Air Water 37(10):776–786

Arıca MY, Kacar Y, Genç Ö (2001) Entrapment of *white-rot fungus Trametes versicolor* in Ca-alginate beads: preparation and biosorption kinetic analysis for cadmium removal from an aqueous solution. Bioresour Technol 80(2):121–129

Bayramoğlu G, Tuzun I, Celik G, Yilmaz M, Arica MY (2006) Biosorption of mercury (II), cadmium (II) and lead (II) ions from aqueous system by microalgae *Chlamydomonas reinhardtii* immobilized in alginate beads. Int J Miner Process 81(1):35–43

Borowiak-Resterna A, Cierpiszewski R, Prochaska K (2010) Kinetic and equilibrium studies of the removal of cadmium ions from acidic chloride solutions by hydrophobic pyridinecarboxamide extractants. J Hazard Mater 179(1–3):828–833

Chen JH, Liu QL, Hu SR, Ni JC, He YS (2011) Adsorption mechanism of Cu (II) ions from aqueous solution by glutaraldehyde crosslinked humic acid-immobilized sodium alginate porous membrane adsorbent. Chem Eng J 173(2):511–519

Çolak F, Atar N, Yazıcıoğlu D, Olgun A (2011) Biosorption of lead from aqueous solutions by *Bacillus strains* possessing heavy-metal resistance. Chem Eng J 173(2):422–428

Dai J, Yan H, Yang H, Cheng R (2010) Simple method for preparation of chitosan/poly(acrylic acid) blending hydrogel beads and adsorption of copper(II) from aqueous solutions. Chem Eng J 165(1):240–249

Eloussaief M, Benzina M (2010) Efficiency of natural and acid-activated clays in the removal of Pb(II) from aqueous solutions. J Hazard Mater 78(1–3):753–757

El-Sayed MT (2013) Removal of lead (II) by *Saccharomyces cerevisiae* AUMC 3875. Ann Microbiol 63:1459–1470

Fan T, Liu Y, Feng B, Zeng G, Yang C, Zhou M, Zhou H, Tan Z, Wang X (2008) Biosorption of cadmium(II), zinc(II) and lead(II) by *Penicillium simplicissimum*: isotherms, kinetics and thermodynamics. J Hazard Mater 160(2–3):655–661

Fenice M, Federici F, Selbmann L, Petruccioli M (2000) Repeated-batch production of pigments by immobilised *Monascus purpureus*. J Biotechnol 80(3):271–276

Fu F, Wang Q (2011) Removal of heavy metal ions from wastewaters: a review. J Environ Manage 92(3):407–418

Futalan CM, Kan C-C, Dalida ML, Hsien K-J, Pascua C, Wan M-W (2011) Comparative and competitive adsorption of copper, lead, and nickel using chitosan immobilized on bentonite. Carbohydr Polym 83(2):528–536

Gerbino E, Mobili P, Tymczyszyn E, Fausto R, Gómez-Zavaglia A (2011) FTIR spectroscopy structural analysis of the interaction between *Lactobacillus* kefir S-layers and metal ions. J Mol Struct 987(1–3):186–192

He ZL, Yang XE, Stoffella PJ (2005) Trace elements in agroecosystems and impacts on the environment. J Trace Elem Med Biol 19(2–3):125–140

Hunsom M, Pruksathorn K, Damronglerd S, Vergnes H, Duverneuil P (2005) Electrochemical treatment of heavy metals (Cu^{2+}, Cr^{6+}, Ni^{2+}) from industrial effluent and modeling of copper reduction. Water Res 39(4):610–616

Juarez Jimenez B, Reboleiro Rivas P, Gonzalez Lopez J, Pesciaroli C, Barghini P, Fenice M (2012) Immobilization of *Delftia tsuruhatensis* in macro-porous cellulose and biodegradation of phenolic compounds in repeated batch process. J Biotechnol 157(1):148–153

Kobya M (2004) Adsorption, kinetic and equilibrium studies of Cr (VI) by hazelnut shell activated carbon. Adsorpt Sci Technol 22(1):51–64

Kumar R, Bishnoi NR, Garima BK (2008) Biosorption of chromium(VI) from aqueous solution and electroplating wastewater using fungal biomass. Chem Eng J 135(3):202–208

Kumar R, Singh R, Kumar N, Bishnoi K, Bishnoi NR (2009) Response surface methodology approach for optimization of biosorption process for removal of Cr (VI), Ni (II) and Zn (II) ions by immobilized bacterial biomass sp. *Bacillus brevis*. Chem Eng J 146(3):401–407

Liu Y, Zhao Q, Cheng G, Xu H (2011) Exploring the mechanism of lead (II) adsorption from aqueous solution on ammonium citrate modified spent *Lentinus edodes*. Chem Eng J 173(3):792–800

Moreno-Piraján JC, Gómez-Cruz R, García-Cuello VS, Giraldo L (2010) Binary system Cu(II)/Pb(II) adsorption on activated carbon obtained by pyrolysis of cow bone study. J Anal Appl Pyrolysis 89(1):122–128

Munagapati VS, Yarramuthi V, Nadavala SK, Alla SR, Abburi K (2010) Biosorption of Cu (II), Cd (II) and Pb (II) by *Acacia leucocephala*

bark powder: kinetics, equilibrium and thermodynamics. Chem Eng J 157(2):357–365

Murugesan A, Ravikumar L, SathyaSelvaBala V, SenthilKumar P, Vidhyadevi T, Kirupha SD, Kalaivani SS, Krithiga S, Sivanesan S (2011) Removal of Pb(II), Cu(II) and Cd(II) ions from aqueous solution using polyazomethineamides: equilibrium and kinetic approach. Desalination 271(1–3):199–208

Nassar MM, Ewida KT, Ebrahiem EE, Magdy YH, Mheaedi MH (2004) Adsorption of iron and manganese ions using low-cost materials as adsorbents. Adsorpt Sci Technol 22(1):25–37

Özdemir S, Kilinc E, Poli A, Nicolaus B, Güven K (2009) Biosorption of Cd, Cu, Ni, Mn and Zn from aqueous solutions by thermophilic bacteria, *Geobacillus toebii* sub.sp. *decanicus* and *Geobacillus thermoleovorans* sub.sp. *stromboliensis*: equilibrium, kinetic and thermodynamic studies. Chem Eng J 152(1):195–206

Ozturk A (2007) Removal of nickel from aqueous solution by the bacterium *Bacillus thuringiensis*. J Hazard Mater 147(1–2):518–523

Rajeshwari K, Kumar MS, Thajuddin N (2012) Adsorption isotherms for Cr (VI) by two immobilized marine cyanobacteria. Ann Microbiol 62(1):241–246

Saurav K, Kannabiran K (2011) Biosorption of Cr (III) and Cr (VI) by *Streptomyces* VITSVK9 spp. Ann Microbiol 61(4):833–841

Soylak M, Erdogan ND (2006) Copper(II)–rubeanic acid coprecipitation system for separation–preconcentration of trace metal ions in environmental samples for their flame atomic absorption spectrometric determinations. J Hazard Mater 137(2):1035–1041

Uluozlu OD, Tuzen M, Mendil D, Soylak M (2010) Coprecipitation of trace elements with Ni^{2+}/2-Nitroso-1-naphthol-4-sulfonic acid and their determination by flame atomic absorption spectrometry. J Hazard Mater 176(1–3):1032–1037

Vijayaraghavan K, Yun Y-S (2008) Bacterial biosorbents and biosorption. Biotechnol Adv 26(3):266–291

Vijayaraghavan K, Teo TT, Balasubramanian R, Joshi UM (2009) Application of Sargassum biomass to remove heavy metal ions from synthetic multi-metal solutions and urban storm water runoff. J Hazard Mater 164(2–3):1019–1023

Yan C, Li G, Xue P, Wei Q, Li Q (2010) Competitive effect of Cu (II) and Zn (II) on the biosorption of lead (II) by *Myriophyllum spicatum*. J Hazard Mater 179(1):721–728

Yang Q, Kocherginsky NM (2006) Copper recovery and spent ammoniacal etchant regeneration based on hollow fiber supported liquid membrane technology: from bench-scale to pilot-scale tests. J Membr Sci 286(1–2):301–309

Zhang X, Su H, Tan T, Xiao G (2011) Study of thermodynamics and dynamics of removing Cu(II) by biosorption membrane of *Penicillium biomass*. J Hazard Mater 193:1–9

Zhao X, Zhang G, Jia Q, Zhao C, Zhou W, Li W (2011) Adsorption of Cu(II), Pb(II), Co(II), Ni(II), and Cd(II) from aqueous solution by poly(aryl ether ketone) containing pendant carboxyl groups (PEK-L): equilibrium, kinetics, and thermodynamics. Chem Eng J 171(1):152–158